Pergamon

PII: S0022-3697(96)00056-X

J. Phys. Chem Solids Vol 58, No. 4, pp. 665–670, 1997

0022-3697/97 $17.00 + 0.00

A SIMULATED ANNEALING STUDY OF CATION DISTRIBUTION IN DEHYDRATED Na-EXCHANGED FAUJASITE ZEOLITES

BAOHUI LI, PINGCHUAN SUN, QINGHUA JIN, JINGZHONG WANG and DATONG DING

Nankai University, Tianjin, 300071, P.R. China

(*Received* 19 *September* 1995; *accepted* 22 *January* 1996)

Abstract—A simulated annealing method is employed to study the cation distribution in dehydrated Na-exchanged faujasite zeolites. By use of the same three parameters, i.e. $e_{I'}-e_I$, $e_{II}-e_I$, the site energy level differences between the cations on the different cation sites I, I′ and II, and w, the repulsive energy between cation pairs located on adjacent sites I and I′, the cation distribution in dehydrated NaHY-type zeolites (with a Si/Al ratio of 2.46) with varying cation loading or temperatures could be accurately predicted. These parameters were determined by fitting the simulated results with experimental data report in the literature. It is found that the influence of the framework Al content, $\overline{N_{Al}}$, on the site energy level differences can be expressed as $e_{I'}-e_I = -23.0490 + 0.5605\overline{N_{Al}}$ KJ mol^{-1} and $e_{II}-e_I = -22.4770 + 0.4437\overline{N_{Al}}$ KJ mol^{-1}. By use of these linear relations and a refined $w = 40$ KJ mol^{-1}, the cation distribution of dehydrated Na-exchanged faujasite with various Al content could be predicted excellently.

Keywords: A. faujasite zeolites, C. simulated annealing, D. cation distribution

1. INTRODUCTION

The exchangeable cations in zeolites have received a great deal of attention in the scientific literature. Thermal stability, sorptive and catalytic properties are all related to the type and number of exchangeable cations and their distribution over the available sites.

X-ray diffraction (XRD) has been, and is, the first-choice technique used in experimental studies of cation locations [1]. In almost all cases, the XRD experiments were carried out at room temperature, perhaps due to technical difficulties. The influence of the temperature has been neglected for a long time [2].

Temperature dependent cation distribution in zeolites was studied in terms of the high temperature X-ray diffractometer camera, which furnished important experimental information and brought about some key developments in theoretical studies.

A statistical thermodynamical model was developed and applied to the study of the cation distributions in zeolites by Van Dun and Mortier [3, 4]. The model's ability to consider the repulsive interactions between the exchangeable cations instead of treating them independently, as in the original Boltzmann-type formalism [5], might explain its success.

Up until now, the statistical thermodynamical model has been successfully used in studies of the influences of temperature, cation loading, different types of exchangeable cations and isomorphous substitution on the cation distribution in faujasite-type zeolites [4, 6, 7]. Recently, the model has been further applied to other types of zeolites [8, 9].

In this paper, the cation distribution in the exchange cation positions of the dehydrated faujasite is studied in terms of the simulated annealing method (a standard Monte Carlo finite temperature technique) [10]. The system being studied is considered as a composition of the framework and contained exchange cations, which is in thermal contact with a heat bath of temperature T. Any possible arrangement of all the contained cations, the location of the cations in the exchange cation sites, corresponds to a certain configuration, or sample, of the system. By use of the simulated annealing approach, a canonical ensemble sample space, i.e. a large collection of configurations, in which the number of the configurations possessing total energy of E^{TOT} is proportional to the Boltzmann factor $\exp(-E^{TOT}/k_BT)$ [11], can be set up efficiently. Since the numbers of cations located in the different types of site can be counted for each configuration, respectively, the populated fractions of sites in equilibrium are then obtained by taking an average from the sample space.

In comparison with the statistical thermodynamical model [3], the simulated annealing method produces results numerically and straightforwardly and does not involve the quasi-chemical equilibrium or the Bragg–Williams approximation treatments as in the analytical discussions. The approximation of the

present study may stem from the fact that the size of the simulation space is not large enough to reproduce the realities of statistical behavior due to the limitation of the computer speed.

2. METHOD

The negative framework charge of zeolites is balanced by cations distributed among energetically different sites. A schematic representation of the faujasite-type structure and the cation sites is shown in Fig. 1. Using Smith's notation [12], the cations in faujasite-type zeolites are distributed over a limited number of sites: the sites I in the center of the hexagonal prism (16 per unit cell); the sites I′ inside the cubo-octahedron opposite one of the hexagonal prism six-membered rings (32 per unit cell); sites II and II′ share the six-membered ring of the cubo-octahedron facing the large cavity-sites II′ inside the cubo-octahedron and sites II in the large cage (II′ is generally only occupied by small adsorbent molecules).

The number of potential cation sites usually exceeds the number of cations to be located. Evidently the equilibrium distribution of the cations over the available sites will be the result of a free energy minimization. In order to make a concrete analysis upon the populated fractions of those sites for the equilibrium state, Monte Carlo simulation is a suitable approach as it adequately studies different structural aspects in the problems of substitutional disorder in solids.

Simulated annealing [10] is known as a global optimization method, which is able to locate efficiently the available configurations of a system at the request of the minimum free energy. It has been successfully used in the simulation of Si, Al distribution of zeolites [13, 14] and has shown its theoretical value for revealing the microscopic underlies of the macroscopic quantities.

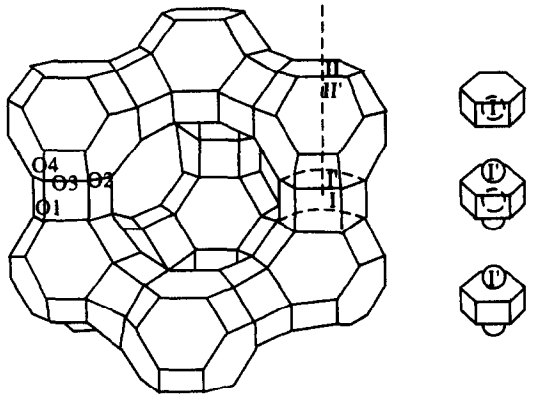

Fig. 1. Framework structure of faujasite-type zeolites with the four different oxygen types (1,2,3,4) and the location of the sites I, I′, II and II′.

To simulate the distribution of cations in the available sites of faujasite, the following assumptions are made:

(1) For lower cation loadings, it is assumed that the cations are located only at three different sites, i.e. site I, I′ and II, amounting to a maximum of 80 coordination sites per unit cell. Indeed all sodium cations are always found in this three sites in Y-type zeolites. However, since simultaneous occupation of cations on adjacent sites I and I′ does not occur [1], the number of cations located at the three sites are at most 64 per unit cell.

For higher cation loadings, occupancy of the site III ($48f$, at the four rings in the supercages) has to be assumed. Therefore, when the number of cations exceeds the limit 64, in our treatment, those surplus cations are located at site III.

(2) $2^3 = 8$ unit cells composed of $B = 640$ exchange cation sites ($B_{\mathrm{I}} = 128$, $B_{\mathrm{I}'} = 256$ and $B_{\mathrm{II}} = 256$) with cyclic boundary conditions considered as a representative portion, or simulation space, of the Na-exchanged faujasites, by which the statistical properties of zeolites are simulated. In this simulated system, the cation number, N, is determined by the given cation loading of the structure being studied. Any one arrangement of N cations ($N = 64 \times 8$ when $N \geq 64 \times 8$, the surplus cations are located on site III) on 640 potential cation sites forms a certain configuration of the system, in which the numbers of cations located on different type of sites, N_i, $i = \mathrm{I}, \mathrm{I}'$ or II, are countable. The populated fractions ($P_i = N_i/B_i$)'s, can then be deduced.

However, only a few energetically favorable configurations can describe efficiently the equilibrium state (under given temperature). The simulated annealing procedure is employed to find those efficient configurations.

(3) In simulated annealing procedure, the energy of the system is considered as an objective function making the quantitative measurement of the degree of the optimization. The energy of a certain configuration of the system is well-defined by the numbers of the cation on the three sites, N_i and the corresponding stabilization energy of a cation located at i-type site, $-e_i$; as well as the number of the nearest neighbor pairs of sites I and I′, occupied simultaneously by cations and the corresponding repulsive energy between such cation pairs, w.

The simulation procedure starts with a randomly created configuration, in which N cations are randomly positioned in 640 potential sites of the system (by a random number generator). A fictitious melting temperature, T, is chosen and decreased in steps. In each step, the configuration is optimized by enough

times (2×10^5, in our treatment) of iterative reconfigurations. In each reconfiguration, one of the N cations is randomly selected and moved to one of its unoccupied neighbor sites as an attempted disturbance of the configuration. According to the Metropolis algorithm [11], if the energy of the original configuration is decreased by the selected cation moving the disturbed configuration is accepted and used as a new one for the next attempt. Whereas, if the cation moving increases the energy of the original configuration by ΔE, then either the disturbed new one is accepted or the original one is kept for the next attempt, depending upon the probability of $\exp(-\Delta E/k_B T)$ (k_B is the Boltzmann constant).

As T is decreased to the temperature being studied, another 2×10^5 reconfiguration is performed and 2×10^5 configurations produced in sequence are collected. It can be proved [11] that the configurations in such a collection are Boltzmann distributed, i.e. the number of configurations with energy E is proportional to the factor $\exp(-E/k_B T)$. Therefore, the configuration collection obtained in this way is what one needs for the sample space with canonical ensemble characters. The macroscopic quantities, such as P_i's, of the system can be obtained by taking an average from the sample space.

3. RESULTS AND DISCUSSION

In the simulation, the energy level differences $e_{I'}-e_I$, $e_{II}-e_I$ and the repulsive energy w are treated as adjustable trial numbers, which are determined through trial and error by matching the calculated numerical results with the literature experimental data.

3.1. *Variation of cation distributions with temperature and cation loading*

Variation of cation populated fractions for the sites I, I′ and II as a function of temperature in $Na_{23}HY$ (with a Si/Al ratio of 2.46, i.e., $Na_{23}H_{32.5}Al_{55.5}Si_{136.5}O_{384}$) is studied by the simulated annealing method. By trial and error, we found that the following setting values of the three parameters, $e_{I'}-e_I = 8.06\,\mathrm{KJ\,mol^{-1}}$, $e_{II}-e_I = 2.15\,\mathrm{KJ\,mol^{-1}}$ and $w \geq 26\,\mathrm{KJ\,mol^{-1}}$, brings the simulated numerical results to a satisfactory fit with the experimental data (see Fig. 2). In Fig. 2 we show the variation of the populated fractions for the sites I, I′ and II as a function of temperature for $Na_{23}HY$, where the lines represent the numerical results obtained by the present simulation and the symbols represent corresponding experimental data quoted from Ref. [4].

Variation of cation populated fractions for the different types of site P_I, $P_{I'}$ and P_{II} as a function of the average number of cations per unit cell ($\bar{N}$) for Na_xHY with a given Si/Al ratio of 2.46 (i.e. $Na_xH_{55.5-x}Al_{55.5}Si_{136.5}O_{384}$) at a temperature of 323 K is also calculated with the setting values mentioned above. In Fig. 3 the P_I, $P_{I'}$ and P_{II} variations

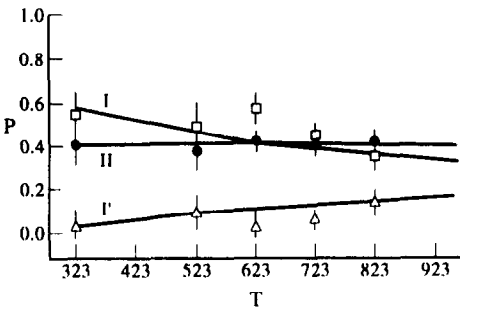

Fig. 2. Variation of the populated fractions for the sites I, I′ and II as a function of temperature for $Na_{23}HY$, compared with literature data [4] (□, site I; △, site I′; ●, site II). Vertical lines represent the standard deviation of each data point [4].

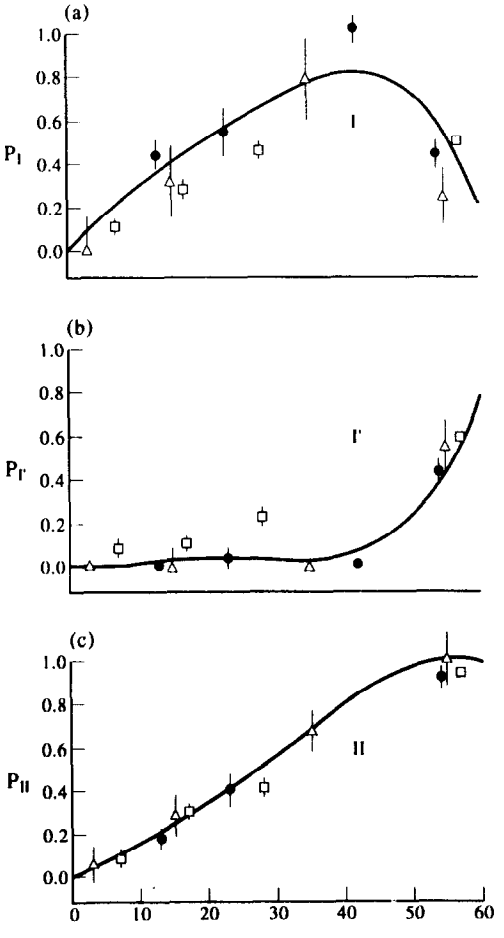

Fig. 3. Variation of the populated fractions for the sites I, I′ and II at 323 K for Na_xHY (Si/Al = 2.46) as a function of the average number of cations per unit cell ($\bar{N}$), compared with literature data: ●, [4]; □, [15]; △, [16]. Vertical lines represent the standard deviation of each data point, quoted from the same literature as the corresponding data points. (a) The sites I; (b) the sites I′; (c) the sites II.

with Na-ion content ($\bar{N}$) are plotted. In order to compare the calculated results with experiments, the corresponding experimental data quoted from Refs [4, 15, 16] are marked with symbols in Fig. 3(a)–(c).

Both studies demonstrate that the Na-ion distribution can be predicted satisfactorily over a wide range of Na-ion content as well as temperature by using three constant parameters ($e_{I'}-e_I$, $e_{II}-e_I$ and w). The energetic site preference series in dehydrated Na_xHY is I > II > I′, resulting in the order of the populated fraction of the sites, $P_I > P_{II} > P_{I'}$, at lower cation loadings. When the cation content increases, the increase of populated fractions P_I and $P_{I'}$ is obstructed by avoiding the follow-up presence of the pair cations locating at adjacent I–I′ sites, due to the strong repulsive interactions between cations of such a pair. Therefore, the site II becomes the most populated one ($P_{II} > P_I$ and $P_{I'}$) at high cation loadings.

3.2. *Cation distribution influenced by Al content*

The site stabilization energy will primarily be determined by the short-range cation–oxygen repulsive interaction which depends upon both the cation itself (radius, charge) as well as the residual negative charge on oxygen. The latter will change with the substitution of Si by Al or the change of framework charge density. In fact, a cation in site I is surrounded by twice as many T-atoms as cations in sites I′ or II, it is expected that the isomorphous substitution of Si by Al is not to affect each site equally and so the site energy level differences have to change with the Si/Al ratio.

Van Dun *et al.* have suggested that the site energy level differences vary with the average number of Al-atoms per unit cell, $\overline{N_{Al}}$ linearly [6], i.e.

$$e_{I'}-e_I = (e_{I'}-e_I)^0 + C\overline{N_{Al}} \quad (1)$$

$$e_{II}-e_I = (e_{II}-e_I)^0 + C\overline{N_{Al}} \quad (2)$$

Equations (1) and (2) are able to explain a site preference reversal from I > II > I′ to II > I′ > I as Si/Al ratio changing from low to high.

Taking notice that site I′ and II are not located equivalently in the structure, a further difference between the slopes of the linear dependence is expected. Therefore, in the present study, the following linear relations are suggested:

$$e_{I'}-e_I = (e_{I'}-e_I)^0 + C_1\overline{N_{Al}} \quad (3)$$

$$e_{II}-e_I = (e_{II}-e_I)^0 + C_2\overline{N_{Al}} \quad (4)$$

where two gradients, C_1 and C_2, are introduced instead of being treated as the same C.

We have found for high-silica faujasite-type zeolites

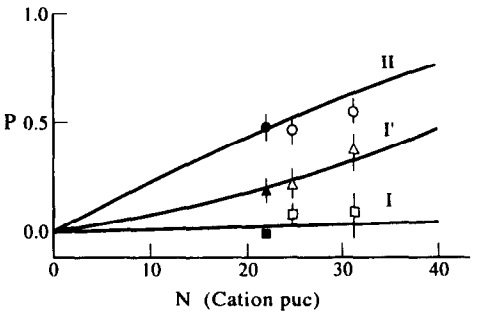

Fig. 4. Variation of the populated fractions for the sites I, I′ and II as a function of temperature for $Na_xH_{32.5-x}Al_{32.5}Si_{159.5}$, compared with literature data [6] (full symbols) and [7] (open symbols) (□, site I; △, site I′; ○, site II). Vertical lines represent the standard deviation of each data point, quoted from the same literature as the corresponding data points.

of $Na_xH_{32.5-x}Al_{32.5}Si_{159.5}O_{384}$, the site populated fractions for all the samples, $x = 22$, 24.8 and 31.2 (experimental data quoted from Ref. [6, 7], respectively), can be predicted nicely (see Fig. 4) with the site energy level differences $e_{I'}-e_I = -4.84\,KJ\,mol^{-1}$, $e_{II}-e_I = -8.06\,KJ\,mol^{-1}$ ($w \geq 26$) instead the $e_{I'}-e_I = 8.06\,KJ\,mol^{-1}$, $e_{II}-e_I = 2.15\,KJ\,mol^{-1}$ for the low-silica case, Si/Al = 2.46, mentioned above.

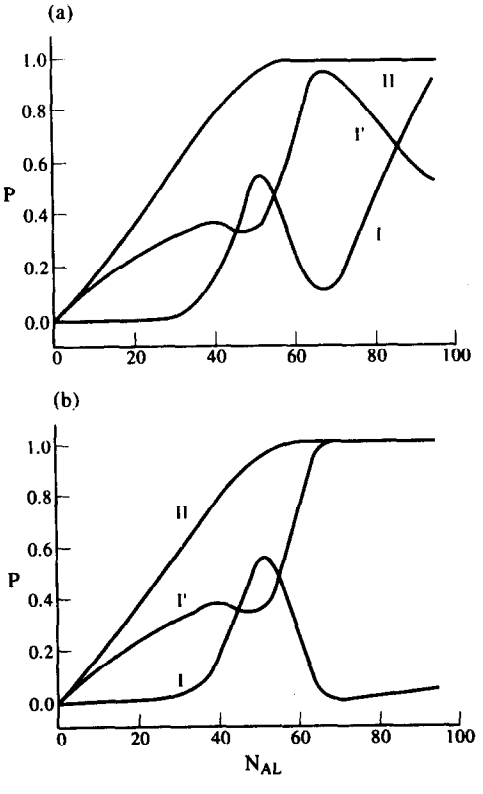

Fig. 5. The variation of the site populated fractions P_I, $P_{I'}$ and P_{II} as a function of $\overline{N_{Al}}$, the site energy level differences $e_{I'}-e_I = -23.0490 + 0.5605\overline{N_{Al}}\,KJ\,mol^{-1}$ and $e_{II}-e_I = -22.4770 + 0.4437\overline{N_{Al}}\,KJ\,mol^{-1}$ are used. (a) $w = 26\,KJ\,mol^{-1}$ and (b) $w = 80\,KJ\,mol^{-1}$.

The parameters in Eqns (3) and (4) $(e_{I'}-e_I)^0 = -23.0490$ $(e_{II}-e_I)^0 = -22.4770$, $C_1 = 0.5605$ and $C_2 = 0.4437$ are then determined by an optimum fitting between the simulated numerical results and literature data for both the low-silica (Si/Al ~ 2.46) and the high-silica (Si/Al ~ 4.9) samples.

3.3. *Refinement of the value of repulsive interaction parameter* w

If the adjacent sites I and I′ can never be occupied simultaneously, the $P_I + P_{I'}$ will not be more than one—implying that w is large enough to be treated as infinity. In our model, this leads to P_I being zero at higher Al-content ($\overline{N_{Al}} > 64$). Nevertheless, this might not be always the case, as some experiments reported (when $\overline{N_{Al}} > 80$, for instance) formerly [17, 18] and recently [19]. In fact, we need not be involved in the argument experimentally. Motivated by the theoretical consideration that for a disordered system, minority energy unfavored events are allowable, we pretested the variations of P_I, P_{II} and $P_{I'}$ as a function of $\overline{N_{Al}}$ under $w = 26$ and $80\,\mathrm{KJ\,mol^{-1}}$, respectively (see Fig. 5). In the calculation, the site energy level differences are determined according to Eqns (3) and (4) and a temperature of 323 K is adopted. It can be seen from Fig. 5 that the calculated results are not sensitive to the setting values of w for $\overline{N_{Al}} < 60$. In comparison with the literature's experimental data [16–21] for the higher Al-content ($\overline{N_{Al}} > 60$), the $w = 26\,\mathrm{KJ\,mol^{-1}}$ setting results in an underestimated P_I and an overestimated $P_{I'}$; whereas the $w = 80\,\mathrm{KJ\,mol^{-1}}$ setting results in the contrary. Therefore, it seems that a modest setting of w will bring about an optimum fitting between the calculated results and the available experimental data over a wider range of Al content.

The optimum results are obtained by using $e_{I'}-e_I = -23.0490 + 0.5605\overline{N_{Al}}\,\mathrm{KJ\,mol^{-1}}$, $e_{II}-e_I = -22.4770 + 0.4437\overline{N_{Al}}\,\mathrm{KJ\,mol^{-1}}$ and a refined $w = 40\,\mathrm{KJ\,mol^{-1}}$. In Fig. 6 the calculated P_I, $P_{I'}$ and P_{II} variations with $\overline{N_{Al}}$ are illustrated by lines and the corresponding experimental data [10–21] are marked with symbols.

In the range of $\overline{N_{Al}} = 0$–32, P_I remains at zero, while both $P_{I'}$ and P_{II} increase with $\overline{N_{Al}}$. In the range of $\overline{N_{Al}} = 32$–48, P_I increases steeply and reaches a maximum $P_I \sim 0.6$ at $\overline{N_{Al}} = 48$; P_{II} increases continuously to its full occupation, $P_{II} \sim 1.0$ at $\overline{N_{Al}} = 48$

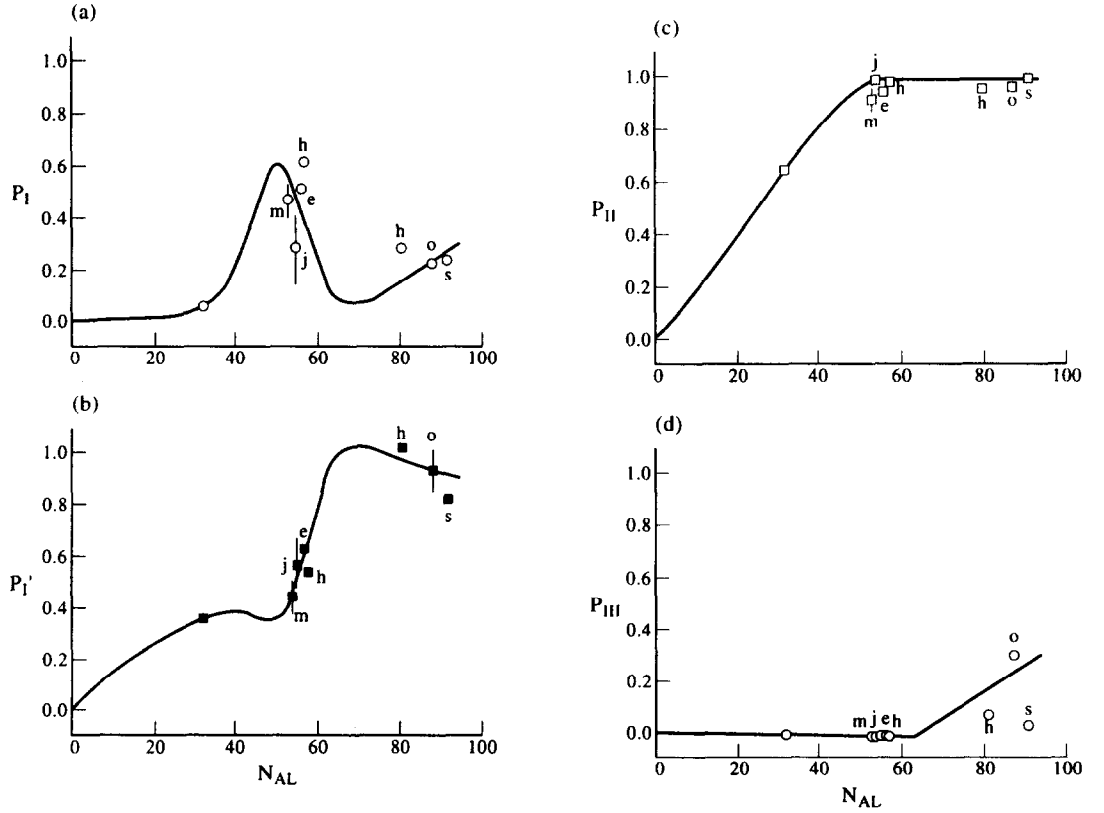

Fig. 6. The predicted variations at 323 K of the site populated fractions as a function of $\overline{N_{Al}}$, compared with literature data, where the subscripts are referred to as: j, Jirak *et al.* [16] s, Smolin *et al.* [17]; h, Hseu [18]; o, Olson [19]; e, Eulenberger *et al.* [20]; m, Mortier *et al.* [21]; and vertical lines represent the standard deviation of the corresponding data points. In this figure the calculated values for $\overline{N_{Al}} = 32.5$ are also plotted. The variation of sites I, I′, II and III is given in Fig. 6(a), (b), (c) and (d), respectively.

and keeps up for $\overline{N_{Al}} > 48$. In the range of $\overline{N_{Al}} = 48-64$, both the decreases of P_I and the increase of $P_{I'}$ with $\overline{N_{Al}}$ are steep. For $\overline{N_{Al}}$ more than 64, according to the model consideration, the surplus Na-cations are positioned forcedly on site III, which results in a linear increase of P_{III} the $P_{I'}$ decreases and the P_I increases again.

4. CONCLUSION

The present study follows the foundation of the statistical thermodynamical model developed by Van Dun *et al.* and has demonstrated that the cation distribution in dehydrated Na-exchanged-faujasite-type zeolites can be satisfactorily predicted by simulated annealing method with varying cation loading and Si/Al ratio. In this method, the statistical quantities of a system in equilibrium are obtained numerically and straightforwardly. Therefore, the present approach is able to avoid the type of approximate treatments typically employed in the analytic expression of the partition function of the system. The significance of the present approach is that the simulated annealing method takes its sampling directly from the structure of the zeolite being studied, and so this approach is beyond the restriction (for faujasite like structure, the quasi-chemical-equilibrium method, which was expected to be better quality than Bragg–Williams approximation by Mortier and Van Dun [4], is successful in that the I′–I–I′ group in the structure can be treated as isolated in space) from the type of the zeolite structure. By Monte Carlo simulation, the study can be easily extended to different types of zeolite. In order to make a rigorous judgement for the present phenomenological study, more experimental data with accuracy are needed.

REFERENCES

1. Mortier W. J., '*Compilation of Extra Framework Site in Zeolites*', Butterworth, Guildford, U.K. (1982).
2. Van Dun J. J. and Mortier W. J., *Zeolites* **7,** 528 (1987).
3. Van Dun J. J. and Mortier W. J., *J. Phys. Chem.* **92,** 6740 (1988).
4. Van Dun J. J., Dhaeze K. and Mortier W. J., *J. Phys. Chem.* **92,** 6747 (1988).
5. Mortier W. J., *J. Phys. Chem.* **79,** 1447 (1975).
6. Van Dun J. J., Dhaeze K., Mortier W. J. and Vaughan D. E. W., *J. Phys. Chem., Solids* **50,** 469 (1989).
7. Lievens J. L., Mortier W. J. and Chao K. J., *J. Phys. Chem., Solids* **53,** 1163 (1992).
8. Lievens J. L., Verduijn J. P., Mortier W. J. and Chao K. J., *Zeolites* **12,** 690 (1992).
9. Lievens J. L., Verduijn J. P., Bons A. J. and Mortier W. J., *Zeolites* **12,** 698 (1992).
10. Kirkpatrick S., Gelatt C. D., Jr. and Vecchi M. P., *Science* **220,** 671 (1983).
11. Metropolis N., Rosenbluth A. W., Rosenbluth M. N., Teller A. H. and Teller E., *J. Phys. Chem.* **21,** 1087 (1953).
12. Smith J. V., '*Molecular Sieves I, ACS Advances in Chemistry Series*', Washington D.C., p. 171 (1971).
13. Herrero C. P., *J. Phys. Chem.* **95,** 3282 (1991).
14. Ding D., Li B., Sun P., Jin Q. and Wang J., *Zeolites* **15,** 569 (1995).
15. Gallezot P. and Imelik B., *J. Chim. Physique Physico-Chim. Biol.* **68,** 816 (1975).
16. Jirak Z., Vratislav S. and Bosacek V., *J. Phys. Chem., Solids* **41,** 1089 (1980).
17. Smolin Y. I., Shepelev Y. F., Butikova I. K. and Petranovskii V. P., *Soviet Phys. Crystallogr.* **28,** 36 (1983).
18. Hseu T. D., Ph.D. thesis, University of Washington (1972). University Microfilms, No. 73-13835 Ann Arbor, Michigan, U.S.A.
19. Olson D. H., *Zeolites* **15,** 439 (1995).
20. Eulenberger G. R., Shoemaker D. P. and Keil J. G., *J. Phys. Chem.* **71,** 1812 (1967).
21. Mortier W. J., Van den Bossche E. and Uytterhoeven J. B., *Zeolites* **4,** 41 (1984).